

# Osteomalacia associated with aluminum intoxication in a patient with chronic renal failure<sup>1</sup>

Thomas W. Bauer, M.D., Ph.D.  
Kathryn L. Popowniak, M.D.  
Bernard N. Stulberg, M.D.  
James T. McMahon, Ph.D.

**Renal osteodystrophy and continual bone pain developed after excision of hyperplastic parathyroid glands in a 51-year-old woman with chronic renal failure. She was found to have osteomalacia associated with aluminum, which was identified at the boundary between mineralized bone and osteoid on biopsy of the iliac crest. Potential use of bone biopsy in such cases is discussed.**

**Index terms:** Aluminum, poisoning • Osteomalacia • Pathology features • Renal osteodystrophy

**Cleve Clin Q 52:271-278, Summer 1985**

Renal osteodystrophy often develops in patients undergoing hemodialysis for chronic renal failure. This is a complicated lesion having histological characteristics of osteitis fibrosa, osteomalacia, or both. Clinical differentiation between the two components can be difficult, and can be

confused further by the presence of osteomalacia associated with aluminum toxicity. We present a case of severe osteomalacia related to aluminum toxicity and discuss the use of bone biopsy in the differential diagnosis.

## Case Report

This 51-year-old woman was well until 21 years prior to admission, when lethargy, swelling of the legs, and hypertension developed and proliferative glomerulonephritis was detected. She was treated with antihypertensive medication and did well until 1979, when chronic renal failure required hemodialysis. Laboratory values are summarized (*Table 1*). A cadaver transplant was rejected and had to be removed after one month, with the patient being maintained on hemodialysis since that time. In 1980, she presented to another hospital with a mass in her breast which proved to be intraductal carcinoma. She was treated with tylectomy and postoperative radiation therapy. In 1982, a 4-cm soft-tissue mass developed in her right shoulder. Radiographs revealed a calcified peri-articular mass consistent with dystrophic calcification. She was then taking folic acid, ferrous sulfate, supplemental calcium, and an antacid which contained aluminum. Over the next two years, the soft-tissue calcification progressed and bone pain gradually developed. During follow-up at another hospital nine months prior to admission, she was found to have serum C-terminal/mid-region parathyroid hormone (PTH) level of 28,415 pg/mL (normal 60-450), and intact/mid-region PTH of 1,495 pg/mL (normal 70-330) with a serum calcium level of 10.6 mg/dL. On presentation eight months prior to her most recent admission, she was found to have severe renal osteo-

<sup>1</sup> Departments of Pathology (T.W.B., J.T.M.), Nephrology (K.L.P.), and Orthopedic Surgery (B.N.S.), The Cleveland Clinic Foundation. Submitted for publication Jan 1985; accepted Mar 1985. sjh

0009-8787/85/02/0271/08/\$3.00/0

Copyright © 1985, The Cleveland Clinic Foundation

**Table 1.** Laboratory values

	Calcium (mg/dL) (normal range 8.5–10.5)	Phosphorus (mg/dL) (normal range 2.4–4.5)	Alkaline Phosphatase (IU/L) (normal range 30–115)
1979	8.7	4.3	—
1980	10.5	8.0	—
1982	10.6	8.7	—
1983	9.5	11.8	314
1984	11.6	8.8	163
1984*	9.5	3.8	—

\* After parathyroidectomy

dystrophy associated with secondary hyperparathyroidism and soft-tissue calcification. At surgery, four hyperplastic parathyroid glands were excised and parathyroid tissue was implanted into the right sternocleidomastoid muscle. Two months later, she was seen as an outpatient complaining of persistent bone pain which was most prominent over the ribs on the right. Serum N-terminal parathyroid hormone was 21 pg/mL (within the reference range) and serum aluminum was 47.2 µg/mL (normal 5–50). On admission, presenting complaints included progressive bone pain, most prominent over the right 10th rib. On physical examination, she was well-developed and well-nourished, with palpable soft-tissue calcifications on the dorsum of each hand and on the right shoulder. Hemoglobin was 8.5 g/dL with a mean corpuscular volume (MCV) of 82.6 fL and a mean corpuscular hemoglobin (MCH) of 27.3 pg. Radiographs showed healing microfractures of the ribs without clear evidence of an underlying lytic lesion. A bone scan showed increased uptake bilaterally in the ribs, as well as in the sacroiliac joints and left proximal femur. The clinical impression was either metastatic carcinoma of the breast or osteomalacia, possibly related to aluminum toxicity, and the right tenth rib and right iliac crest were biopsied. In order to facilitate recognition of actively mineralizing bone, the patient was given oxytetracycline over a three-day period starting two weeks before the biopsy, followed by demeclocycline for three days starting five days before the biopsy.

Iliac crest biopsy was performed at a standardized location 2 cm postero-inferior to the antero-superior iliac spine. A transverse sample which contained both outer and inner cortical tables of the pelvis, encompassing the trabecular (medullary) bone, was obtained using an 8-mm trocar,

sleeve, and biopsy needle. The rib specimen was decalcified, processed using routine histological methods, and stained with hematoxylin and eosin. The iliac crest sample was fixed in 70% ethyl alcohol, processed for non-decalcified staining, sectioned using a Jung microtome, and stained with hematoxylin and eosin, Goldner's trichrome, and toluidine blue. In addition, aurine tricarboxylic acid stain for aluminum was applied as described by Maloney et al,<sup>1</sup> and Prussian blue stain for iron was applied according to standard histological methods. Quantitation of selected parameters of bone remodeling was determined using a digitizing pad and Apple IIE microcomputer with appropriate software (R&M Biometrics, Nashville, Tenn). The results are presented (Table 2). For electron microscopy, 10-µ sections of non-decalcified iliac crest bone cut on a Jung microtome were mounted on standard glass slides or graphite wafers and deplasticized. For transmission electron microscopy, inverted Beem capsules were placed over appropriate bone sections on the slides, filled with Spurr resin, and polymerized with heat. Capsules were warmed in an oven and snapped free of the glass by immersion in liquid nitrogen. Thin sections were cut at 60–80 nm and viewed under a Philips 400 TEM/STEM with no prior osmium post-fixation or staining. For scanning electron microscopy uncoated bone sections on graphite wafers were examined using a back-scatter electron detector. Energy-dispersive x-ray analysis was conducted on specimens prepared for both scanning and transmission electron microscopy using an EDAX x-ray detector having a 30-mm<sup>2</sup> detection window. Semiquantification of iron and aluminum was conducted by area counting of elemental dot maps prepared by single-channel analysis of x-ray spectra gathered at both mineralized bone/osteoid and osteoid/bone-marrow interfaces. The data were tabulated in graphic form and correlated with representative sections of bone osteoid.

The routinely processed, decalcified rib specimen showed essentially unremarkable fragments of cortical and trabecular bone. Though such decalcified specimens facilitate sectioning, the process also prohibits histological identification of unmineralized bone (osteoid). While decalcification rules out the possibility of diagnosing osteomalacia on routinely processed bone samples, this type of specimen was sufficient to exclude metastatic carcinoma in our patient. The iliac crest sample (Fig. 1) was processed without decalcification and demonstrated marked osteomalacia. The cortex was approximately normal in thickness, but showed increased porosity, suggesting previous episodes of hyperparathyroidism. The total volume of trabecular bone was somewhat decreased (Table 1), and there was a marked increase in the amount of unmineralized bone, diagnostic of osteomalacia. No tetracycline labels were seen on fluorescent microscopy, providing further evidence of a severe mineralization defect. There was no evidence of increased active resorption of bone (osteoclasts), and paratrabecular fibrosis was absent. These findings were also consistent with clinical evidence of normalized parathyroid hormone levels. Staining for aluminum showed prominent deposition along the mineralization front (Fig. 2), the interface between osteoid and mineralized bone. These histological findings were diagnostic of aluminum toxicity associated with osteomalacia. In addition, stains for iron showed prominent deposition along the marrow-osteoid interface (Fig. 3). Using scanning electron microscopy, the distal osteoid bordering

**Table 2.** Results of bone histomorphometry

	Patient	Normal*
Trabecular bone volume	14.1%	(22.5%)
Trabecular osteoid surface	88.0%	(18.9%)
Trabecular osteoid area	37.4%	(1.9%)
Mean osteoid seam width	37.3 µm	(9.7 µm)
Osteoclasts/mm trabecular surface	0	(0.03)
Area of marrow fibrosis	0	(0%)
Trabecular surface tetracycline labeled	0	(12.87%)

\* Normal values adapted, in part, from Vigorita.<sup>20</sup>



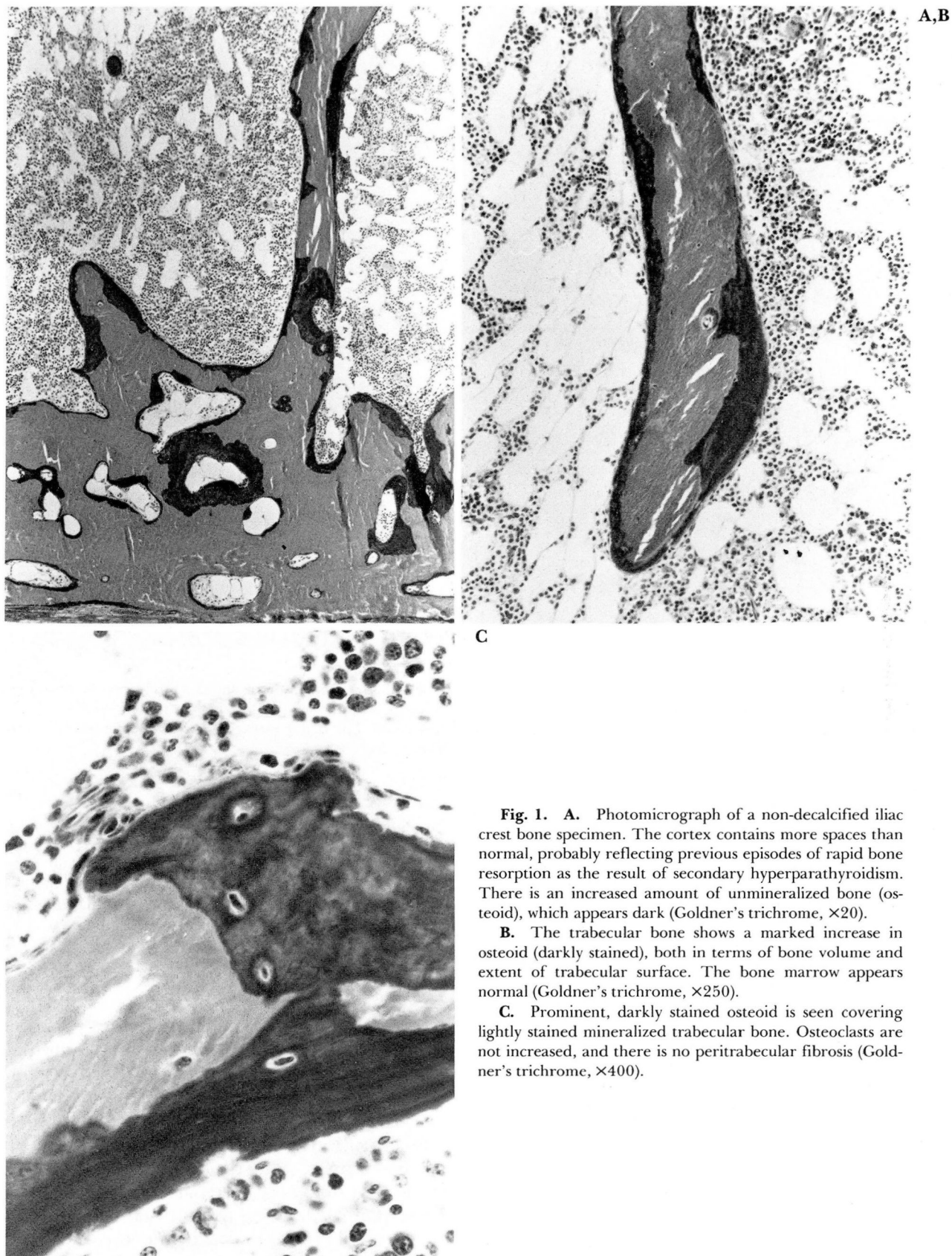


**Fig. 1. A.** Photomicrograph of a non-decalcified iliac crest bone specimen. The cortex contains more spaces than normal, probably reflecting previous episodes of rapid bone resorption as the result of secondary hyperparathyroidism. There is an increased amount of unmineralized bone (osteoid), which appears dark (Goldner's trichrome,  $\times 20$ ).

**B.** The trabecular bone shows a marked increase in osteoid (darkly stained), both in terms of bone volume and extent of trabecular surface. The bone marrow appears normal (Goldner's trichrome,  $\times 250$ ).

**C.** Prominent, darkly stained osteoid is seen covering lightly stained mineralized trabecular bone. Osteoclasts are not increased, and there is no peritrabecular fibrosis (Goldner's trichrome,  $\times 400$ ).



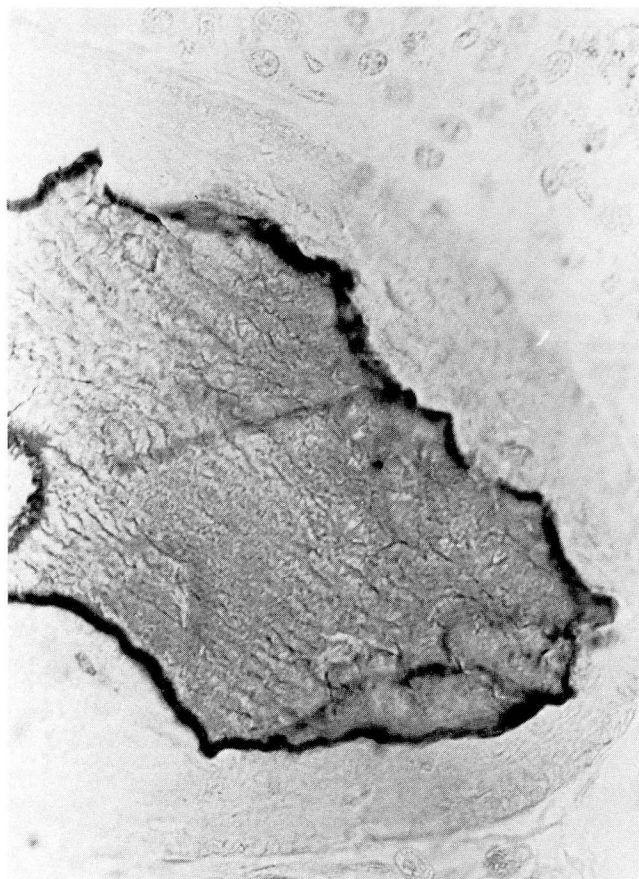


**Fig. 2.** Staining for aluminum shows a prominent band along the mineralization front, corresponding to the line between the pale-stained osteoid and the darker mineralized bone (aluminum,  $\times 400$ ).



**Fig. 3.** Staining for iron shows a positive band along the marrow-osteoid interface (arrow). Iron is present within the marrow histiocytes, but is not markedly increased (not shown) (Prussian blue,  $\times 400$ ).

the marrow was lined by a bright band several microns wide, while the proximal border at the mineralized front showed a similar band when demonstrated using backscattered electrons (*Fig. 4A*). Since backscatter electron imaging is particularly sensitive to variations in atomic density, these bands were thought to correspond to areas of altered mineralization. Area dot maps of proximal and distal osteoid demonstrated fairly well-defined linear accumulations of aluminum and iron respectively, along the mineralized bone and bone-marrow interface as illustrated by their graphic representations (*Fig. 4, B and C*) and also corresponding to their appearance on light microscopy. Transmission electron microscopy of similar osteoid segments revealed a 3- to 5- $\mu$ -wide band of electron-dense particles within the osteoid component bordering the mineralized bone interface (*Fig. 5*). These particles measured 275–300 nm in diameter and were characterized by a dense central core with dense crystalline projections at the periphery (*Fig. 5, inset A*). X-ray analysis of these particles revealed an elemental composition of aluminum, calcium, phosphorus, and magnesium (*Fig. 6A*). Although confined principally to the proximal osteoid margin, a few particles having a similar composition were

also identified within the mineralized component of the bone. The distal osteoid near the bone-marrow interface contained an ill-defined band composed of fine granules that appeared to be clustered between collagen fibrils (*Fig. 5, inset B*). These particles had x-ray spectral values indicating the presence of iron, as well as small amounts of calcium, phosphorus, silicon, sulfur, and chlorine (*Fig. 6B*).

## Discussion

The potential toxicity of aluminum accumulation in patients undergoing chronic hemodialysis was recognized in the early 1970s with the appearance of “dialysis dementia,” a neurological syndrome which appears to be related to high concentrations of aluminum in the gray matter of the brain.<sup>2,3</sup> Shortly thereafter, it was recognized that many of these patients also suffer from bone pain, fractures, and muscle weakness, particularly when the dialysate is prepared from tap



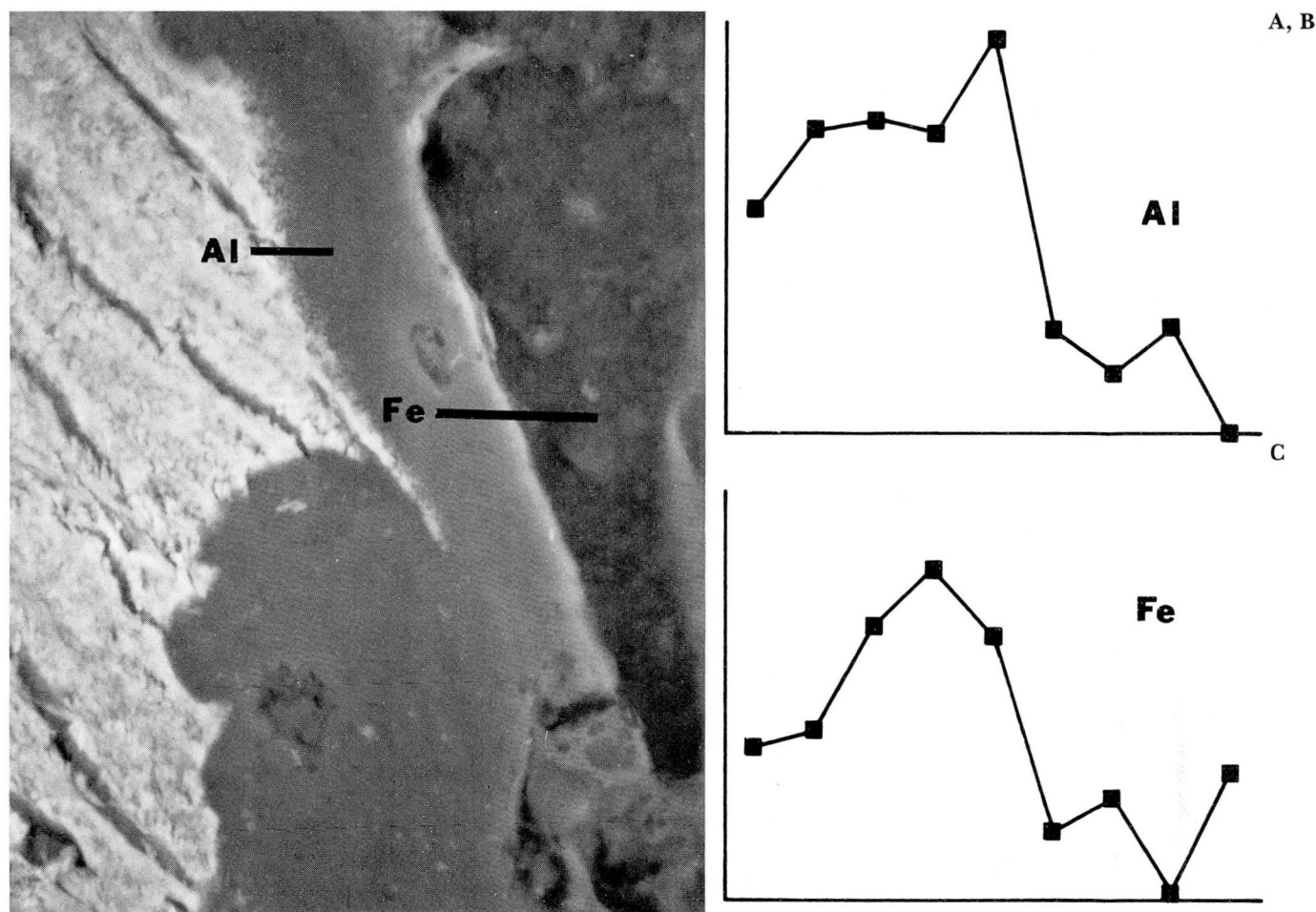


**Fig. 4.** A. Scanning electron micrograph using back scatter electron imaging of trabecular bone segments. The osteoid matrix appears thickened and homogeneous, with several vascular spaces. The bright bands at the mineralized bone/osteoid and osteoid/bone-marrow interfaces may represent abnormal zones of mineralization (unstained,  $\times 800$ ). Al = aluminum and Fe = iron.

B. Graphic representation of aluminum in the regions bordering the mineralized bone/osteoid interface. Representative areas of analysis are depicted by the line crossing the mineralization front in A. Aluminum concentration is highest within the osteoid component nearest the mineralization front.

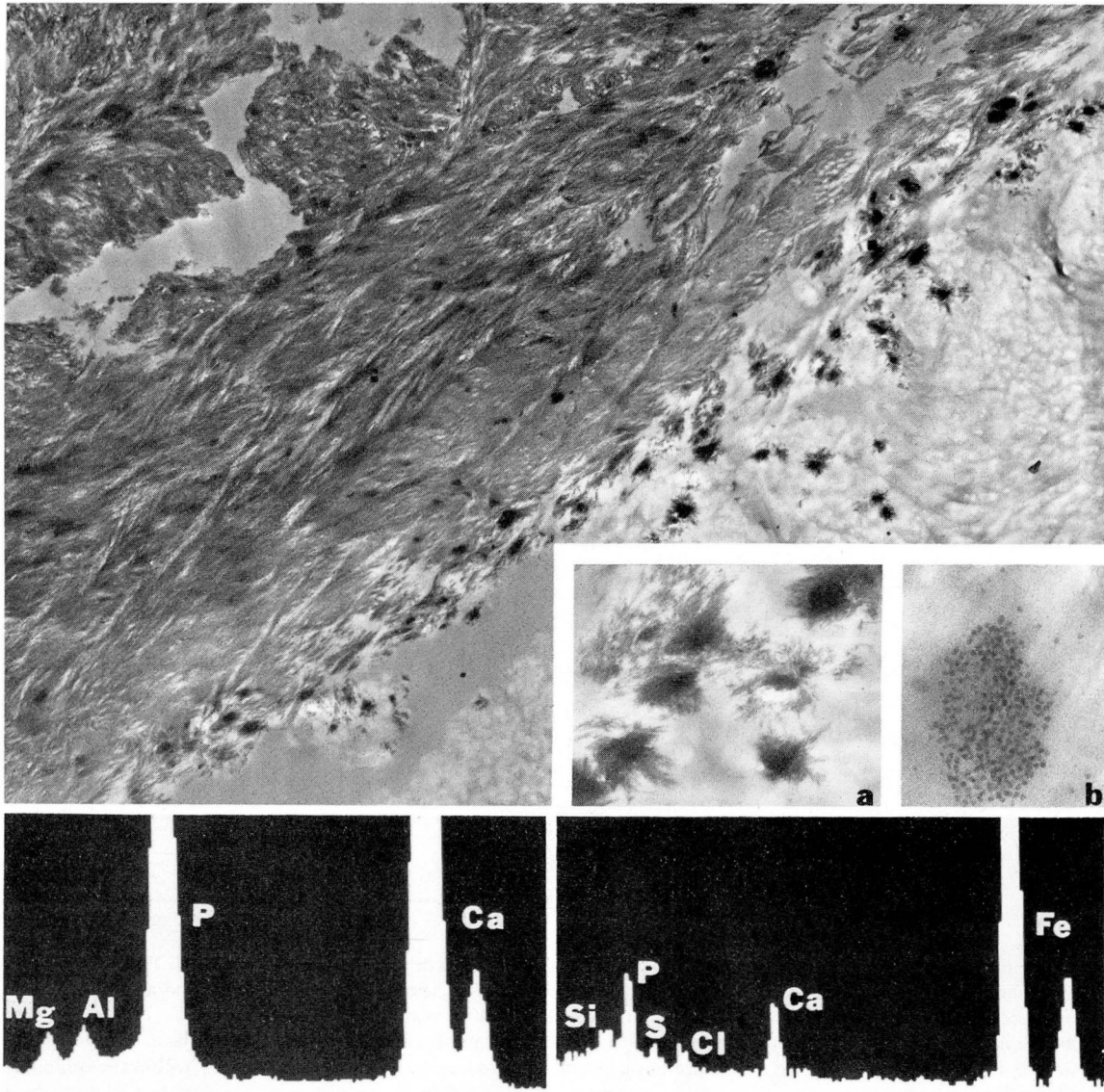
C. Graphic representation of iron in the areas bordering the osteoid/bone-marrow interface. Representative areas of analysis are depicted by the line crossing the outside edge of the osteoid in A. Iron concentration is highest adjacent to the osteoid/marrow interface.

water containing large amounts of aluminum. There was also a marked reduction in the incidence of dialysis encephalopathy and osteomalacia when deionized water was used instead.<sup>4,5</sup> Once the potential for aluminum toxicity from dialysate water had been recognized, standards for aluminum levels were developed and the incidence of encephalopathy and osteomalacia decreased; however, osteomalacia continued to be reported in patients ingesting phosphate-binding antacids which contained aluminum. Increased accumulation of aluminum in bone is now rec-

ognized as common in patients undergoing renal hemodialysis who take antacids that contain aluminum.<sup>6</sup> Aluminum deposits have been identified histologically in 44% of patients undergoing long-term dialysis<sup>7</sup> and 20% of patients with primarily osteomalacic renal osteodystrophy.<sup>8</sup> Although it is difficult to prove that aluminum is causally related to osteomalacia, a number of observations suggest a pathogenetic role. These include (a) concentration of aluminum along the mineralization front with a lack of tetracycline labeling, (b) correlation between the extent of



5



6A, B

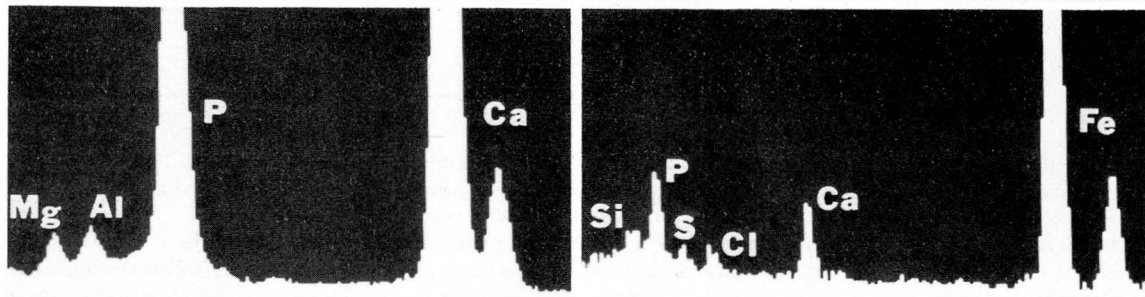


**Fig. 5.** Transmission electron micrograph of the mineralization front in a trabecular bone segment. A band of variably spaced electron-dense particles is seen within the osteoid component bordering the mineralized bone/osteoid interface (unstained,  $\times 7,000$ ). At higher magnification (inset **a**), the particles demonstrate dense cores with crystalline projections at the periphery (unstained,  $\times 22,000$ ). Another micrograph (inset **b**) shows the fine granular particles found in areas bordering the osteoid/bone marrow interface. They are frequently clustered between collagen fibrils (unstained,  $\times 80,000$ ).

**Fig. 6. A.** X-ray analysis of particles seen in **Figure 4A**. They are composed of aluminum, calcium, phosphorus, and magnesium.

**B.** X-ray analysis of the fine granular particles seen in inset **b** of **Figure 5**. They contain a high concentration of iron and lesser concentrations of calcium, phosphorus, silicon, sulfur, and chlorine.

aluminum staining and other histomorphometric parameters of a mineralization defect,<sup>9,10</sup> (c) the epidemiologic correlation between osteomalacia and aluminum content in dialysate water,<sup>2</sup> (d) the decreased incidence of osteomalacia, coupled

with an increased number of calcification fronts and reduction in stained bone aluminum when deionized water is used in dialysis,<sup>11,12</sup> and (e) the decrease in stained bone aluminum following treatment of patients with deferoxamine.<sup>7</sup> In ad-

dition, aluminum intoxication and osteomalacia have been reported in patients with uremia but not on dialysis<sup>13</sup> and in patients being treated with total parenteral nutrition without dialysis.<sup>8</sup> Normal individuals who ingest phosphate-binding gels containing aluminum can excrete 0.5 mg of aluminum in their urine each day.<sup>6</sup> If renal function is reduced, however, aluminum gradually accumulates in bone, and with rapid aluminum loading, serum, liver, and brain concentrations increase, leading to toxicity.<sup>6,14</sup>

Histochemical staining for aluminum in non-decalcified bone has been found to be accurate. The relative extent of bone staining for aluminum correlates well with the amount of bone aluminum detected by atomic absorption spectrophotometry ( $r = 0.81-0.955$ ),<sup>1,15</sup> although the staining technique is not as sensitive as atomic absorption. Ott et al<sup>15</sup> found that bone staining was negative when aluminum content was found to be 20–50 mg/kg by atomic absorption. Since the upper limit of normal for bone aluminum was considered to be 8 mg/kg, the authors suggested that any aluminum detected by histochemical staining is abnormal. The location of aluminum staining within the bone is identical to that demonstrated using analytical ion microscopy.<sup>9</sup>

Previous studies have documented the presence of aluminum in the general region of the mineralization front.<sup>10</sup> Our x-ray analysis demonstrated aluminum within the osteoid, with a particularly high concentration adjacent to the mineralized bone.

At least two studies have suggested that deferoxamine might be beneficial in the treatment of aluminum toxicity.<sup>7,16</sup> This chelating agent leads to a transient increase in serum aluminum, facilitating removal of the deferoxamine-aluminum complex through dialysis. The temporary increase in serum aluminum after deferoxamine infusion may also be a useful test for detecting elevated bone levels. However, Malluche et al<sup>7</sup> found that while all 12 patients studied with histologically documented elevated bone aluminum showed increased serum aluminum after deferoxamine infusion, elevation was also seen in 4 out of 10 patients without aluminum-associated osteomalacia.

While the importance of detecting aluminum in the blood and bone of patients taking antacids is well recognized, the significance of increased stainable iron within osteoid is much less clear.<sup>17</sup> Patients with chronic renal failure often have

normochromic normocytic anemia, due in part to decreased erythropoietin production. Blood loss during venipuncture for dialysis and laboratory studies also contributes to anemia, and it has become customary to replace iron stores in such patients. However, standards for iron administration are not clear, and it has been suggested that the serum ferritin and red cell indexes, especially MCV and MCH, are the best criteria of iron metabolism in patients on chronic hemodialysis.<sup>18</sup> Bone-marrow biopsy can also demonstrate iron; however, the specimens are usually decalcified before processing, making evaluation of osteoid impossible. In our experience, iron and aluminum commonly (but not always) occur together within osteoid, and the extent and intensity of iron staining in osteoid does not necessarily correlate with bone-marrow iron. Red-cell indexes showing microcytic or normocytic anemia in most patients suggest that iron stores may not be in excess. Gokal et al<sup>18</sup> found that mechanisms that regulate iron absorption are usually intact in such cases and suggested that many dialysis patients receiving routine parenteral iron dextran may be overloaded with iron, while those receiving oral iron probably are not. Iron has also been found within the osteoid of patients with osteomalacia complicating thalassemia and transfusional hemosiderosis.<sup>19</sup> The fact that deferoxamine chelates both iron and aluminum simplifies therapy in a patient with both iron and aluminum associated with osteomalacia, but it may complicate attempts to determine the pathogenic significance of each element.

Thomas W. Bauer, M.D., Ph.D.  
Department of Pathology  
The Cleveland Clinic Foundation  
9500 Euclid Ave.  
Cleveland OH 44106

## References

1. Maloney NA, Ott SM, Alfrey AC, Miller NL, Coburn JW, Sherrard DJ. Histological quantitation of aluminum in iliac bone from patients with renal failure. *J Lab Clin Med* 1982; **99**:206–216.
2. Alfrey AC, Mishell JM, Burks J, et al. Syndrome of dyspraxia and multifocal seizures associated with chronic hemodialysis. *Trans Am Soc Artif Intern Organs* 1972; **18**:257–261.
3. Alfrey AC, LeGendre GR, Kaehny WD. The dialysis encephalopathy syndrome. Possible aluminum intoxication. *N Engl J Med* 1976; **294**:184–188.



4. Pierides AM, Edwards WG Jr, Cullum UX Jr, McCall JT, Ellis HA. Hemodialysis encephalopathy with osteomalacic fractures and muscle weakness. *Kidney Int* 1980; **18**:115-124.
5. Walker GS, Aaron JE, Peacock M, Robinson PJA, Davison AM. Dialysate aluminium concentration and renal bone disease. *Kidney Int* 1982; **21**:411-415.
6. Alfrey AC, Hegg A, Craswell P. Metabolism and toxicity of aluminum in renal failure. *Am J Clin Nutr* 1980; **33**:1509-1516.
7. Malluche HH, Smith AJ, Abreo K, Faugere M. The use of deferoxamine in the management of aluminium accumulation in bone in patients with renal failure. *N Eng J Med* 1984; **311**:140-144.
8. Ott SM, Maloney NA, Coburn JW, Alfrey AC, Sherrard DJ. The prevalence of bone aluminum deposition in renal osteodystrophy and its relation to the response to calcitriol therapy. *N Engl J Med* 1982; **307**:709-713.
9. Cournot-Witmer G, Zingraff J, Plachot JJ, et al. Aluminum localization in bone from hemodialyzed patients: relationship to matrix mineralization. *Kidney Int* 1981; **20**:375-378.
10. McClure J, Smith PS. The localization of aluminium and other elements in bone tissue of a case of renal osteodystrophy with an associated dialysis encephalopathy syndrome. *J Pathol* 1984; **142**:293-299.
11. McClure J, Fazzalari NL, Fassett RG, Pugsley PG. Changes in bone histoquantitative parameters and histochemical staining reactions for aluminium in a group of patients with chronic renal failure following a reduction in the aluminium concentration of the haemodialysis fluid. *J Clin Pathol* 1984; **37**:743-747.
12. Ward MK, Feest TG, Ellis HA, et al. Osteomalacic dialysis osteodystrophy: evidence for a water-borne aetiological agent, probably aluminium. *Lancet* 1978; **1**:841-845.
13. Andreoli SP, Bergstein JM, Sherrard DJ. Aluminum intoxication from aluminum-containing phosphate binders in children with azotemia not undergoing dialysis. *N Engl J Med* 1984; **310**:1079-1084.
14. Klein KL, Maxwell MH. Renal osteodystrophy. *Orthop Clin North Am* 1984; **15**:687-695.
15. Ott SM, Maloney NA, Klein GL, et al. Aluminum is associated with low bone formation in patients receiving chronic parenteral nutrition. *Ann Intern Med* 1983; **98**:910-914.
16. Brown DJ, Dawborn JK, Ham KN, Xipell JM. Treatment of dialysis osteomalacia with desferrioxamine. *Lancet* 1982; **2**:343-345.
17. Pierides AM, Myli MP. Iron and aluminum osteomalacia in hemodialysis patients (letter). *N Engl J Med* 1984; **310**:323.
18. Gokal R, Millard PR, Weatherall DJ, Callender STE, Ledingham JGG, Oliver DO. Iron metabolism in haemodialysis patients. A study of the management of iron therapy and overload. *J Med* 1979; **48**:363-391.
19. De Vernejoul MC, Girot R, Gueris J, et al. Calcium phosphate metabolism and bone disease in patients with homozygous thalassemia. *J Clin Endocrinol Metab* 1982; **54**:276-281.
20. Vigorita VJ. The tissue pathologic features of metabolic bone disease. *Ortho Clin N Amer* 1984; **15**:613-629.